

## Supporting Information

### Voltammetry of monovalent cations at the 2D/3D water interface formed by using a slitlike graphene-membrane nanofluidic device

Zhenmei Yu<sup>#</sup>, Yan Li<sup>#</sup>, Siran Du, Zengtao Zhang, Xiqing Cheng, Qingwei Wang, Yong Chen\*

School of Chemical and Environmental Engineering, Shanghai Institute of Technology (SIT),  
Shanghai 201418, China

<sup>#</sup>Z. Yu and Y. Li contributed equally to this work.

\*Corresponding author: E-mail: [yongchen@sit.edu.cn](mailto:yongchen@sit.edu.cn)

#### 1. Experimental Procedures

##### 1.1 General experimental Materials and chemicals

All the materials and chemicals used to prepare the free-standing graphene laminar membrane (F-GLM) and the physically confined graphene laminar membrane (PC-GLM) are as follows: graphene monolayer nanosheets dispersion (flake size ranging from 0.5 to 3.0  $\mu\text{m}$ , Nanjing XFNANO materials Tech Co., Ltd, China), porous nylon membrane (pore diameter~0.22  $\mu\text{m}$ , membrane diameter~50 mm, CHANGDE BKMAN TECHNOLOGY Co., Ltd, China), and senior silicone gel (BZ Silicones Co., Ltd, China).

The chemicals of KCl, NaCl,  $\text{MgCl}_2$ , LiCl, TMACl, TEACl, TBACl, HCl (36%~38%), isopropanol ( $\geq 99.7\%$ ) are analytical grade (Sinopharm, China). High-resistivity distilled water was used to prepare all aqueous solutions. All the reagents were used as received without any further purification.

##### 1.2 Instrumentation

A laser confocal Raman microscopic spectrometer customized by the Shanghai dalan technology Co., Ltd, China and equipped with an iHR320-Imaging spectrometer (Spectrum: 150-1500 nm, HORIBA) was used for the Raman spectroscopy measurements. The electrochemical experiments were conducted by using an electrochemical workstation (CHI660D, CHI, USA) and

the shielding box (CHI202, CHI, USA), which have widely been employed in our studies on the ion transfer behaviors across the membrane-supported liquid/liquid interface.<sup>1-6</sup>

The apparatus employed in the preparations of F-GLM and PC-GLM mainly include the vacuum filtration pump (HPD-25, Shanghai Mosu Science Equipment Co., Ltd., Shanghai, China) and a high-speed centrifuge (TGL-16C, Shanghai Anting Scientific Instrument Factory, Shanghai, China).

Some instruments were used for the structural and hydrophilic characterizations of as-prepared F-GLM and PC-GLM, mainly including XRD (XRD-6100, SHIMAOZU, Japan), XPS (K-ALPHA, Thermo Fisher Scientific, America), SEM (S-3400N, HITACHI, Japan) and contact angle measurement instrument (SDC-1005, Guangdong Dayt intelligent technology Co., LTD, Guangdong, China).

### **1.3 Preparation of the free-standing graphene laminar membrane (F-GLM)**

Based on our previous work<sup>4</sup> with a few modifications, the setup and the procedure employed in the fabrication of free-standing graphene laminar membrane (F-GLM) by the vacuum filtration method are illustrated as Figure. S1 and described as follows. In brief, 2 mL of commercial 2 g/L n-methyl-2-pyrrolidone (NMP) monolayer graphene nanosheets dispersion was centrifuged at 5500 rpm for 30 minutes. TEM and AFM images of the commercial monolayer graphene nanosheets used in this work are shown as as Figure. S2. The supernatant in the centrifuge tube was carefully removed and the sediment was re-dispersed in 40 mL isopropanol by sonication for 3 minutes to obtain the graphene mono-layered sheet dispersion (~0.1 g/L).

Subsequently, as-prepared monolayer graphene nanosheets dispersion (2.0 mL) was filtered through a porous nylon membrane by vacuum filtration under the pressure of 10 kPa. After that, the porous nylon membrane covered with the graphene laminates was dried at 80°C in an oven overnight, and then immersed in the distilled water (10.0 mL) for 3-5 minutes to peel off the free-standing graphene laminar membrane (F-GLM) from the surface of porous nylon membrane. As-obtained F-GLM was further dried at 80°C in an oven over 24 hours for the followed preparation of physically confined graphene laminar membranes (PC-GLM).

#### **1.4 Preparation of the physically confined graphene laminar membrane (PC-GLM)**

The fabrication procedure of a PC-GLM is shown as Figure. S3a and described as the followed steps: (1) as-prepared F-GLM was cut into some rectangular strips with wideness~1.0 mm and length~2.0 cm; (2) such a F-GLM strip was flatly put between two glass slides coated with the silicone gel (2.0 mL) and then slowly press two glass slides until that the F-GLM strip was completely sealed by the silicone gel; The distance between two glass slides was finally controlled as about 1.0 cm; (3) the F-GLM covered with the silicone gel and glass slides was dried at 80°C in an oven overnight for the complete solidification of silicone gel, and then carefully peeled off the sealed F-GLM from the surfaces of two glass slides and finally cut into a PC-GLM composed of the graphene laminates inside the silicone gel (Figure. S3b-e).

#### **1.5 Fabrication of a slitlike graphene-membrane nanofluidic device and constructing an ion trans-membrane system by using such a nanofluidic device**

Fabrication of a slitlike graphene-membrane nanofluidic device: A PC-GLM with length of 1.0 mm was glued into the middle of a glassy tube (length~6.0 cm, inner diameter~7 mm and outer diameter~8.0 mm), but both of the open ends of PC-GLM was not sealed by the silicone gel. After the complete solidification of silicone gel under 80°C in an oven overnight, a slitlike graphene-membrane nanofluidic device was fabricated (Figure. S4a).

Construction procedure of an ion trans-membrane system by using such a nanofluidic device: A slitlike graphene-membrane nanofluidic device and a 10 mL glass beaker are respectively used as the cell 1 and the cell 2 (Figure. S4b). The chloride solution with same concentration was respectively poured into the cell 1 and cell 2, including HCl, KCl, NaCl, KCl, TMAcI, TEAcI, TBAcI. The four-electrode system was employed in the followed electrochemical experiments by using ion-transfer voltammetry (ITV) including linear scan voltammetry (LSV) and cyclic voltammetry (CV) on the basis of our previous report<sup>1-6</sup>. One pairs of platinum wire electrodes were used as the counter electrodes and two Ag/AgCl wire electrodes were employed as the reference

electrodes (Figure. S4b). After that, an ion trans-membrane system composed of such a nanofluidic device with two bulk aqueous solutions ( $W_{\text{bulk}}$ ) was successfully constructed, that is the  $W_{\text{bulk}}(\text{A})/\text{PC-GLM}/W_{\text{bulk}}(\text{B})$  system as shown in Fig. 1. All the electrochemical measurements were conducted inside a shielding box (CHI202, CHI, USA) (Figure. S4c).

After a F-GLM was used instead of the PC-GLM, the  $W_{\text{bulk}}(\text{A})/\text{F-GLM}/W_{\text{bulk}}(\text{B})$  system was constructed according to our previous work.<sup>4</sup> Noticeably, the ion trans-membrane direction in these two systems are completely different. In the case of  $W_{\text{bulk}}(\text{A})/\text{F-GLM}/W_{\text{bulk}}(\text{B})$  system, the ion trans-membrane direction is perpendicular to the 2D graphene nanochannels of F-GLM. As for the  $W_{\text{bulk}}(\text{A})/\text{PC-GLM}/W_{\text{bulk}}(\text{B})$  system, the ion trans-membrane direction is parallel to the 2D graphene nanochannels of PC-GLM (Figure S4d).

## 2. Supplementary figures

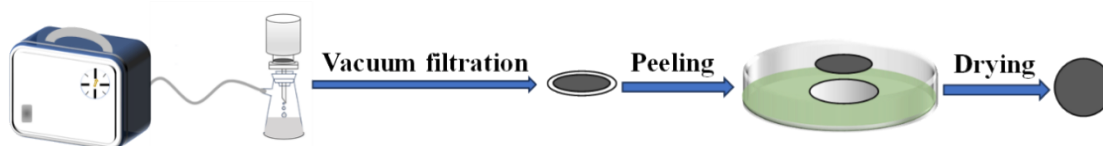


**Figure. S1** Schematic illustration of the fabrication of a free-standing graphene laminar membrane (F-GLM) by using vapor filtration method.

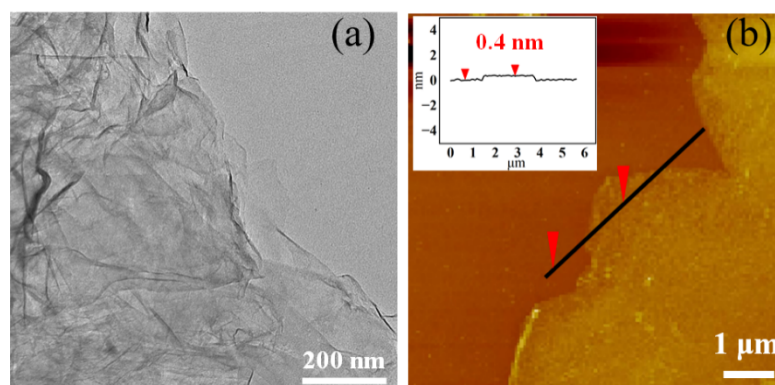


**Figure. S2** TEM (a) and AFM (b) images of the commercial monolayer graphene nanosheets employed for the fabrication of a free-standing graphene laminar membrane (F-GLM) by using

vapor filtration method.

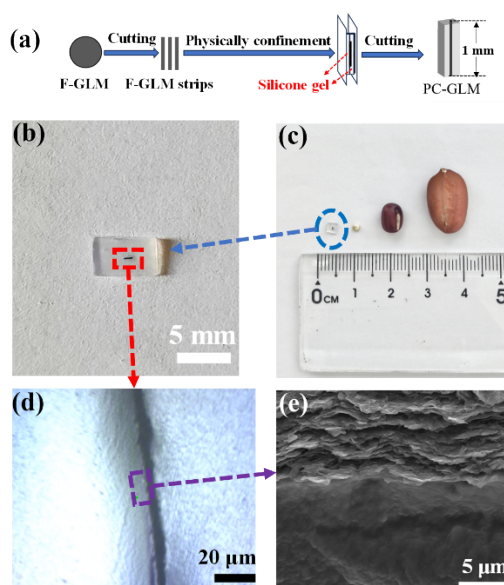


**Figure. S3** (a) Schematic illustrating the fabrication procedure of a physically confined graphene laminar membranes (PC-GLM) by using silicone gel. Photographs of (b) a PC-GLM with length of 1.0 mm and (c) the size of a PC-GLM compared with a sesame seed, an ormosia and a peanut kernel. (d) Micro-image of the cross-sectional area marked by a red rectangle in (b). (e) SEM image of the marked region in (d).

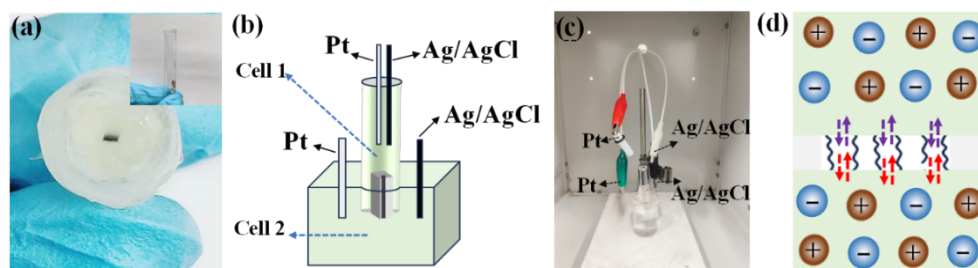


**Figure. S4** The ion trans-membrane system constructed by the combination of such a slitlike graphene-membrane nanofluidic device with two bulk aqueous phases containing various chloride solutions with an identical concentration in cell 1 and cell 2. (a) Photograph of a slitlike graphene-membrane nanofluidic device. (b) Schematic of the  $W_{\text{bulk}}(\text{A})/\text{PC-GLM}/W_{\text{bulk}}(\text{B})$  system containing different chloride salts with the same concentration in cell 1 and cell 2. (c) Photograph of the four-electrode system in an electrochemically shielding box. (d) Schematic of the ion trans-membrane processes of cation and anion along the parallel direction to the 2D graphene nanochannels physically confined by the silicone gel in the slitlike graphene-membrane nanofluidic device.

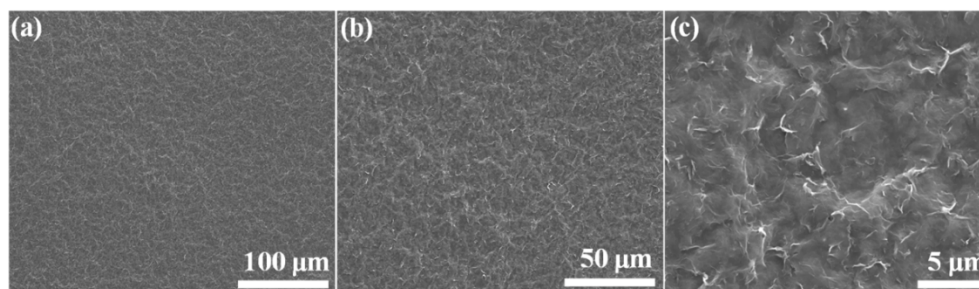


**Figure. S5** Top-viewed SEM images of the F-GLM under different magnification. Some winkles can be seen on the surface of F-GLM, which is similar to those graphene laminar membranes formed on the support.<sup>4</sup>

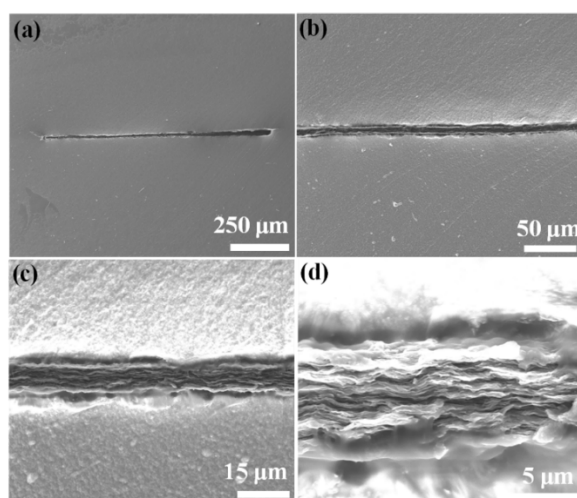


**Figure. S6** Top-viewed SEM images of the PC-GLM under different magnification.

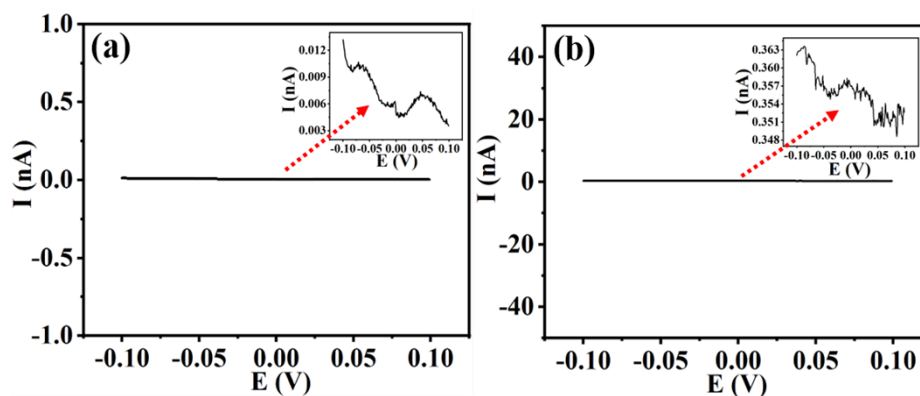


**Figure. S7** Leakage experiments for testing the sealing effect of silicone gel employed in this work. (a) LSV curve obtained by using a glass tube sealed by only silicone gel (device (I)) after 90 days; (b) LSV curve obtained by using a device composed of a strip of polyethylene (PE) membrane without pores instead of the F-GLM strip (device (II)) after 90 days.

Although all of our previous work on the membrane-supported L/L interface have already proven the excellent sealing effect of silicone gel,<sup>1-6</sup> the possible leakage caused by the silicone gel was further tested by using two reference devices without pores. To make sure that the slitlike graphene-membrane nanofluidic device sealed properly and did not allow any leakage or spurious currents, HCl solution (1.0 mM) was employed to test the possible leakage of the devices without the graphene laminar membrane composed of 2D graphene nanochannels inside the silicone gel because proton (diameter~3.4 Å) is the smallest ion in aqueous solution.<sup>7</sup> Figure S7a and 7b show that only the current responses with the level of pA were obtained for the device (I) and device (II) after 90 days, which indicates that the leakage caused by the silicone gel can be neglected.

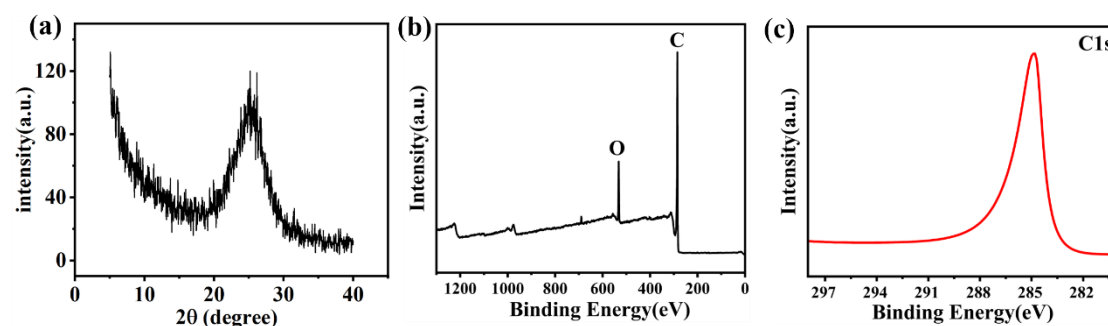


**Figure. S8** (a) The XRD pattern of F-GLM. (b) XPS survey spectra of F-GLM. (c) The C1s spectra of the F-GLM.

Figure S8 (a) shows the XRD pattern of F-GLM and a characteristic diffraction peak presents at 26.5°, which can be assigned to the characteristic diffraction peak of the (002) peak of graphene membranes. The *d*-spacing value of as-prepared F-GLM is calculated to be 0.34 nm according to Bragg equation, which accords to the previous reports.<sup>4,8</sup> In addition, Figure S8 (b) and (c) show the XPS spectra of F-GLM. As-prepared F-GLM presents high C1s at 284.8 eV, but weak O1s at 531.1 eV due to the oxygenic functional groups on the graphene sheet edges, which accords to the XPS characterization results of graphene layers as reported previously.<sup>37, 38</sup>

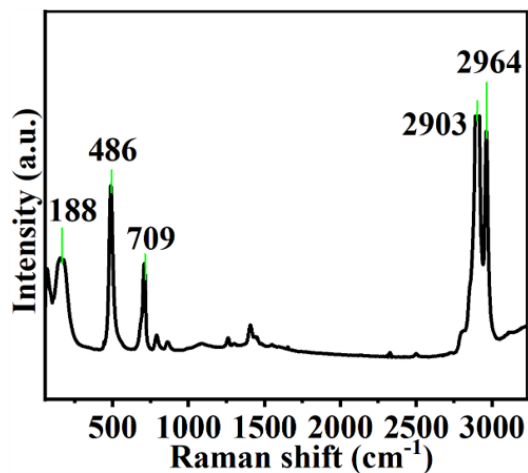


**Figure. S9** The Raman spectrum of the silicone gel used in this work.

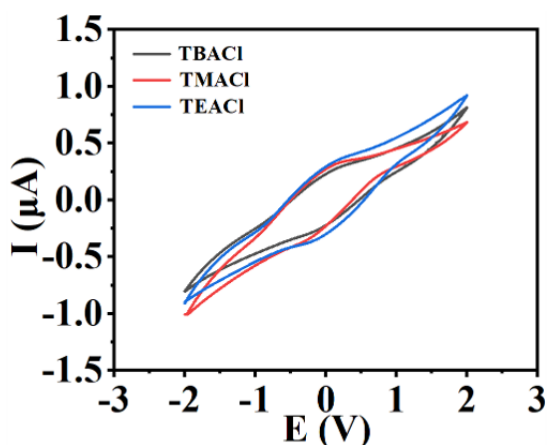


**Figure. S10** The cyclic voltammograms obtained in the ion trans-membrane system of  $W_{\text{bulk}}(\text{A})/\text{PC-GLM}/W_{\text{bulk}}(\text{B})$  by using TMACl, TEACl and TBACl (1.0 mM) in both of  $W_{\text{bulk}}(\text{A})$  and  $W_{\text{bulk}}(\text{B})$ . Scan rate is 40 mV/s.

We investigated the trans-membrane behaviors of some monovalent organic cations with much larger ion diameter (1.25-1.6 nm) than the hydrated ion diameter ( $\sim 0.7$  nm) of  $\text{Li}^+$ ,  $\text{Na}^+$  and  $\text{K}^+$ ,<sup>9</sup> including tetramethylammonium ( $\text{TMA}^+$ ), tetraethylammonium ( $\text{TEA}^+$ ) and tetrabutylammonium ( $\text{TBA}^+$ ). As shown as Figure S10, as-obtained CV curves are almost same to those CVs of  $\text{Li}^+$ ,  $\text{Na}^+$ ,  $\text{K}^+$ , namely no Faradaic response corresponding to the cation transfer can be observed within the remarkably wide potential window (-2.0 V-2.0 V).

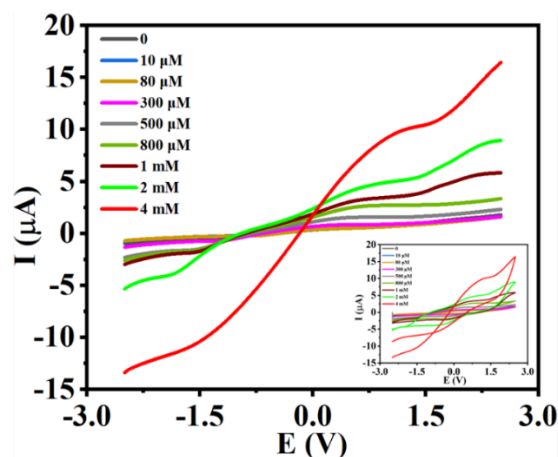


**Figure. S11** (a) LSV and (b) CV curves obtained under the different concentration of proton ( $C_{H^+}$ ) in two bulk aqueous phases ( $W_{bulk}$ ) of the  $W_{bulk}(A)/PC\text{-}GLM/W_{bulk}(B)$  system (the inset is the corresponding CV curves).

Figure S11 shows that the peak currents ( $I_p$ ) of CV and LSV curves increases with the concentration of  $H^+$  in both of aqueous solutions ( $W_{bulk}$ ) and the linear relationship between  $I_p$  and  $C_{(H^+)}$  is about  $300\mu M\text{-}1.0mM$ .

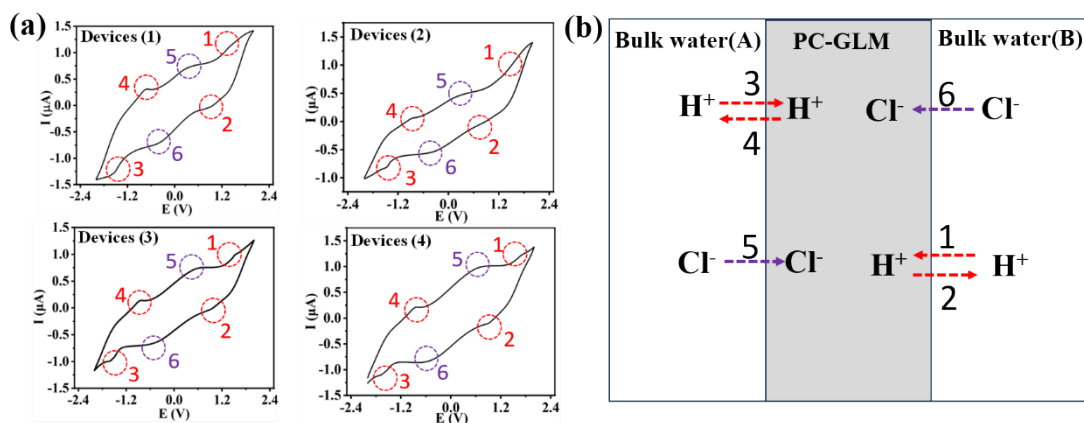


**Figure. S12** (a) The cyclic voltammograms obtained by using four slitlike graphene-membrane nanofluidic devices (Devices (1)-(4)) in the  $W_{bulk}(A)/PC\text{-}GLM/W_{bulk}(B)$  system (1.0 mM HCl in both of  $W_{bulk}(A)$  and  $W_{bulk}(B)$ ). Scan rate is 40 mV/s. (b) The possible mechanism for the peaks 1-6 appearing in those double transfer voltammograms obtained by using those slitlike graphene-membrane nanofluidic devices.

Four slitlike graphene-membrane nanofluidic devices (Devices (1)-(4)) composed of the PC-

GLM with same length of 1.0 mm were fabricated and studied. As shown as Figure S12 (a), the extremely wide potential windows (-2.0 V-2.0 V) and the double transfer voltammograms can also be obtained, which are similar to those CVs as seen in Fig. 3b and the supported liquid membrane (SLM) system.<sup>10-14</sup> The application of electrochemistry to a SLM can be viewed as a bipolar version of liquid/liquid electrochemistry and the cation transfer across an interface in the SLM systems can be coupled with the transfer of an anion across the other interface.<sup>14</sup>

Therefore, the peaks 1-6 appearing in the Fig. 3b and Figure S12 (a) could be attributed to the followed ion transfer processes occurring at the 2D/3D water interface formed between the 2D graphene-nanoconfined water in the PC-GLM (PC-graphene@water) and two bulk aqueous phases ( $W_{\text{bulk}}(A)$  and  $W_{\text{bulk}}(B)$ ). The peak current of peak 4 corresponding to the proton transfer from the PC-graphene@water to the bulk aqueous phase (A) was used to estimate the repeatability of these four slitlike graphene-membrane nanofluidic devices and listed in the Table S2.

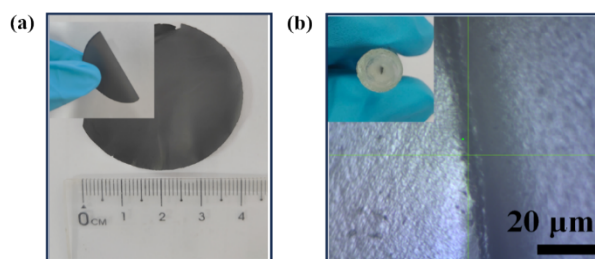
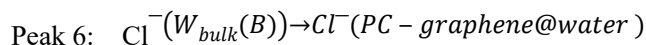
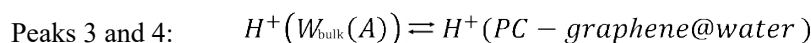
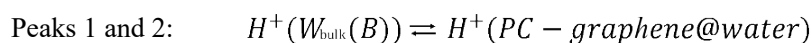


**Figure. S13** (a) The photograph of as-prepared free-standing graphene oxide membrane (F-GOM). (b) The micro-image of physically confined graphene laminar membrane PC-GOM. The insets in the Fig. S13a and b are the photographs of the folded F-GOM and the slitlike graphene oxide membrane nanofluidic device fabricated by using a PC-GOM.

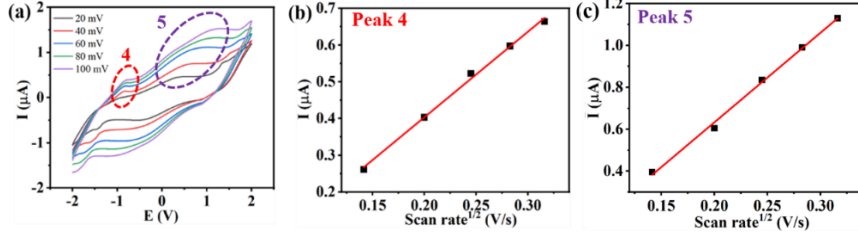


**Figure. S14** (a) CV curves obtained under the different scan rates changing from 20 mV/s to 100 mV/s. The relationships between the peak currents of (b) the peak 4 corresponding to the proton transfer as well as (c) the peak 5 corresponding to the proton transfer and the square root of scan rate ( $v^{1/2}$ ).

As shown as Figure. S14a, the peak currents ( $I_p$ ) of peak 4 and peak 5 corresponding to the proton transfer and the chloride transfer increased with the scan rate. Figure. S14b and c further demonstrate that the values of  $I_p$  of peak 4 and peak 5 are proportional to the square root of scan rate ( $v^{1/2}$ ). According to the modified Randles-Ševčík equation (1) used in the SLM system<sup>11,14</sup>, the diffusion coefficient of proton in the 2D PC-graphene@water is calculated about  $1.64 \pm 0.2 \times 10^{-5} \text{ cm}^2 \text{ s}^{-1}$ , which is smaller than the value ( $9.0 \times 10^{-5} \text{ cm}^2 \text{ s}^{-1}$ ) of proton in bulk water possibly due to the distinct phase behavior of 2D PC-graphene@water from the bulk aqueous phase as discussed in the text. The diffusion coefficient of chloride in the bulk aqueous phase is estimated about  $3.5 \pm 0.2 \times 10^{-5} \text{ cm}^2 \text{ s}^{-1}$ , which is close to the diffusion coefficient ( $4.1 \times 10^{-5} \text{ cm}^2 \text{ s}^{-1}$ ) of chloride in the bulk water as reported previously<sup>15</sup>.

$$I_p = 0.3837 \left( \frac{nF}{RT} \right)^{1/2} nFAD_w^{1/2} C v^{1/2} \quad (1)$$

where  $n$  is the charge number,  $F$  is the farad constant,  $R$  is the gas constant, and  $T$  is the Kelvin temperature (298 K).  $C$  is the concentration of  $\text{H}^+$  in the PC-GLM or  $\text{Cl}^-$  in the bulk aqueous phase. In addition,  $I_p$ ,  $A$  and  $D$  respectively refer to the peak currents of peaks 4 and 5, the efficient area of the 2D/3D water interface and the diffusion coefficients of proton in 2D PC-graphene@water or  $\text{Cl}^-$  in the bulk aqueous phase. If the efficient area of the interface is approximately estimated according to the geometrical area, the  $A$  is evaluated about  $3.0 \times 10^{-5} \text{ cm}^2$  on the basis of the  $d$ -spacing value ( $\sim 3.4 \text{ \AA}$ ) (Figure S8) and the thickness of graphene laminar membrane in the silicone gel ( $\sim 6.0 \text{ \mu m}$ ) (Figure S6).

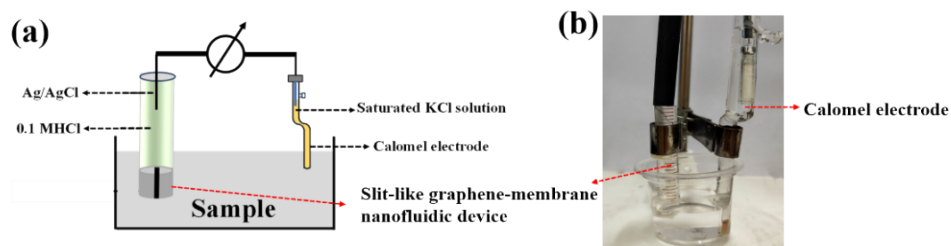


**Figure. S15** (a) The schematic and (b) the photograph of a potentiometric measuring setup fabricated by employing such a slitlike graphene-membrane nanofluidic device.

As shown as Figure S15, a potentiometric measuring setup was fabricated by employing the slitlike graphene-membrane nanofluidic device composed of a PC-GLM. The inner filling solution inside the slitlike graphene-membrane nanofluidic device is 0.1 M HCl. The reference electrode is a commercial calomel electrode ( $\varphi_{\text{ref}}(\text{Hg}_2\text{Cl}_2/\text{Hg}) = 0.28 \text{ V vs SHE}$ , Shanghai LEI CI Co., LTD). We found that the potential is in proportion to the pH values of sample solution within the range of 1.0-4.0, which indicates that such a slitlike graphene-membrane nanofluidic device can play the same role as the SLMs to build the the membrane potential ( $\varphi_{\text{mem}}$ ) composed of two phase boundary potentials ( $\varphi_{\text{inner}}$  and  $\varphi_{\text{outer}}$ ) at the membrane solution interfaces as refined as following formula (2).<sup>10-14</sup>

$$\varphi_{\text{mem}} = \varphi_{\text{inner}} - \varphi_{\text{outer}} = K + \frac{2.303RT}{zF} \lg a_{\text{H}^+} = K - \frac{2.303RT}{zF} \text{pH} \quad (2)$$

The limited linear dependence between the membrane potential and the pH values of the testing solution could be ascribed to the much small volume ( $\approx A (3.0 \times 10^{-5} \text{ cm}^2) \cdot L (0.1 \text{ cm}) : 3.0 \cdot 10^{-3} \mu\text{L}$ ) of 2D graphene-nanoconfined water in the slitlike graphene-membrane nanofluidic device, which may be overcome by the fabrication of slitlike graphene-membrane nanofluidic device composed of slit arrays inside the silicone gel.

**Table. S1** The values of dielectric constant ( $\epsilon$ ), viscosity ( $\eta$ ) and density ( $\rho$ ) of bulk water, some organic solvents and 2D graphene-nanoconfined water under the ambient conditions<sup>7-24</sup>

Solvents	Property	Dielectric	Viscosity	Density
		constant	(mPa·s)	(g/cm <sup>3</sup> )
		12		

Bulk water	78.4 <sup>16</sup>	0.88 <sup>16</sup>	0.998 <sup>16</sup>
1, 2-Dichloroethane (DCE)	10.2 <sup>17</sup>	0.84 <sup>17</sup>	1.24 <sup>17</sup>
Nitrobenzene (NB)	35.15 <sup>18</sup>	1.20 <sup>19</sup>	1.20 <sup>19</sup>
1, 6-Dichlorohexane (DCH)	8.8 <sup>20</sup>	2.04 <sup>21</sup>	1.07 <sup>22</sup>
1,2-Dichlorobenzene (ODCB)	7 ± 2 <sup>23</sup>	2.32 <sup>24</sup>	1.29 <sup>24</sup>
1,9-Decadiene	2.1 <sup>25</sup>	-	-
Nitrophenyl octyl ether (NPOE)	23.9 <sup>26</sup>	12.8 <sup>27</sup>	1.04 <sup>28</sup>
n-Octanol	10.3 <sup>29</sup>	6.25 <sup>29</sup>	0.82 <sup>29</sup>
2D graphene-nanoconfined water inside the nanochannels with height ( $h < 1.0$ nm)	2.1( $\epsilon_{\perp}$ ) <sup>30</sup> ( $h: 0.34$ nm)	3.84 <sup>31</sup> ( $h: 0.68$ nm)	1.7 <sup>32</sup> ( $h: 0.75$ nm)

**Table. S2** The peak currents corresponding to the proton transfer from the 2D PC-graphene@water to the  $W_{\text{bulk}}$ (A) by using four slitlike graphene-membrane nanofluidic devices

	Device (1)	Device (2)	Device (3)	Device (4)
Peak current (nA)	215.2	220	210.8	223

**Table. S3** The diffusion coefficients of proton ( $D_p$ ) obtained under different aqueous environments

Different aqueous environments	$D$ ( $H^+$ ) ( $\text{cm}^2 \text{s}^{-1}$ )	Refs.
Bulk water	$9.0 \times 10^{-5}$	33

Lipid bilayer surface	$5.8 \times 10^{-5}$	34
Water/n-decane interface	$5.7 \pm 0.7 \times 10^{-5}$	35
2D PC-graphene@water	$1.64 \pm 0.2 \times 10^{-5}$	this work
Bio-membrane surface	$1.2 \times 10^{-5}$	36
2D ordered ice phase	$4.0 \times 10^{-6}$	7

## References

- (1) Chen, Y.; Bian, S.; Gao, K.; Cao, Y.; Wu, H.; Liu, C.; Jiang, X.; Sun, X., Studies on the meso-sized selectivity of a novel organic/inorganic hybrid mesoporous silica membrane. *J. Membr. Sci.* **2014**, *457*, 9-18.
- (2) Jiang, X.; Gao, K.; Hu, D.; Wang, H.; Bian, S.; Chen, Y., Ion-transfer voltammetric determination of folic acid at meso-liquid-liquid interface arrays. *Analyst.* **2015**, *140* (8), 2823-2833.
- (3) Gao, K.; Jiang, X.-H.; Hu, D.-P.; Bian, S.-J.; Wang, M.; Chen, Y., Impact of an ionic surfactant on the ion transfer behaviors at meso-liquid/liquid interface arrays. *Chin Chem Lett.* **2015**, *26* (3), 285-288.
- (4) Wang, X.; Yang, H.; Yu, Z.; Zhang, Z.; Chen, Y., Two-Dimensional Graphene-Based Potassium Channels Built at an Oil/Water Interface. *Materials.* **2023**, *16* (15).
- (5) Hu, D.; Wang, H.; Gao, K.; Jiang, X.; Wang, M.; Long, Y.; Chen, Y., Anion transfer across “anion channels” at the liquid/liquid interface modified by anion-exchange membrane. *RSC Adv.* **2014**, *4* (100), 57035-57040.
- (6) Qiu, H.; Jiang, T.; Wang, X.; Zhu, L.; Wang, Q.; Zhao, Y.; Ge, J.; Chen, Y., Electrochemical investigation of adsorption of graphene oxide at an interface between two immiscible electrolyte solutions. *RSC Adv.* **2020**, *10* (43), 25817-25827.
- (7) Gopinadhan K, H. S., Esfandiar A, et al. Complete steric exclusion of ions and proton transport through confined monolayer water. *Science.* **2019**, *363*(6423): 145-148.
- (8) Hirunpinyopas, W.; Iamprasertkun, P.; Bissett, M. A.; Dryfe, R. A. W. Tunable charge/size selective ion sieving with ultrahigh water permeance through laminar graphene membranes. *Carbon.* **2020**, *156*, 119-129.
- (9) A. Esfandiar, B. Radha, F. C. Wang, Q. Yang, S. Hu, S. Garaj, R. R. Nair, A. K. Geim, K. Gopinadhan, *Science*, 2017, **358**, 511-513.
- (10) Parhi, P. K., Supported Liquid Membrane Principle and Its Practices: A Short Review. *J.CHEM.* **2013**, *2013*, 1-11.
- (11) O. Shirai, S. Kihara, Y. Yoshida, M. Matsui. Ion transfer through a liquid membrane or a bilayer lipid membrane in the presence of sufficient electrolytes. *J. Electroanal.* **1995**, *389*(1-2): 61-70.

- (12) Ulmeanu S M, J. H., Samec Z, et al, Cyclic voltammetry of highly hydrophilic ions at a supported liquid membrane. *J. Electroanal.* **2002**, 530(1-2): 10-15.
- (13) Bakker E; B. P.; Pretsch E. Polymer Membrane Ion-Selective Electrodes—What Are the Limits? *Electroanalysis*. **1999**, 11, 915-933.
- (14) Velicky, M.; Tam, K. Y.; Dryfe, R. A., Mechanism of ion transfer in supported liquid membrane systems: electrochemical control over membrane distribution. *Anal Chem.* **2014**, 86 (1), 435-42.
- (15) Lopez Cascales J J, Otero T F. Molecular dynamic simulation of the hydration and diffusion of chloride ions from bulk water to polypyrrole matrix. *J. Chem. Phys.* **2004**, 120(4): 1951-1957.
- (16) Chuangchote, S.; Sagawa, T.; Yoshikawa, S., Electrospinning of poly (vinyl pyrrolidone): Effects of solvents on electrospinnability for the fabrication of poly (p-phenylene vinylene) and TiO<sub>2</sub> nanofibers. *J. Appl. Polym.* **2009**, 114 (5), 2777-2791.
- (17) Hanai T. Dielectric properties of emulsions: III. Dielectric behavior of W/O emulsions. *Kolloid-Zeitschrift*, **1961**, 177: 57-61.
- (18) Powell A L, M. A. E., The Properties of Tetraethylammonium and Tetra-n-butylammonium Picrates in Anisole-Nitrobenzene Solutions. *J. Am. Chem. Soc.* **1957**, 79(9): 2118-2123.
- (19) Rimboud, M.; Elleouet, C.; Quentel, F.; L'Her, M., Potential scale for ion transfers at the water|1,6-dichlorohexane interface. *Electrochim.* **2010**, 55 (7), 2513-2517.
- (20) Katano, H.; Tatsumi, H.; Senda, M., Ion-transfer voltammetry at 1,6-dichlorohexane|water and 1,4-dichlorobutane|water interfaces. *Talanta*. **2004**, 63 (1), 185-93.
- (21) Bochyński Z, D. H., Molecular Correlations in Liquid mono-and Dlichloroalkanes. *Acta Phys. Pol.* **1996**, 89(4): 547-554.
- (22) Snyder C R, D. J. F., Determination of the Dielectric Constant of Nanoparticles. 1. Dielectric Measurements of Buckminsterfullerene Solutions. *J. Phys. Chem. B.* **2000**, 104(47): 11058-11065.
- (23) Felixa S P S, S. K. U., Venis A R, Molecular Interaction Studies on Binary Liquid Mixtures of 1, 2-Dichlorobenzene and Toluene at 308.15 k. *Joseph's College (Autonomous)*.
- (24) Toledano, T.; Biller, A.; Bendikov, T.; Cohen, H.; Vilan, A.; Cahen, D., Controlling Space Charge of Oxide-Free Si by in Situ Modification of Dipolar Alkyl Monolayers. *J. Phys. Chem. C.* **2012**, 116 (21), 11434-11443.
- (25) Sánchez-Pedreño C, O. J. A., Hernández J., Perchlorate-selective polymeric membrane electrode based on a gold (I) complex: application to water and urine analysis. *ANAL CHIM ACTA.* **2000**, 415(1-2): 159-164.
- (26) Garcia-Rodríguez, A.; Matamoros, V.; Kolev, S. D.; Fontàs, C., Development of a polymer inclusion membrane (PIM) for the preconcentration of antibiotics in environmental water samples. *J. Membr. Sci.* **2015**, 492, 32-39.
- (27) Soliman, S. S.; Sedik, G. A.; Elghobashy, M. R.; Zaazaa, H. E.; Saad, A. S., Greenness assessment profile of a QbD screen-printed sensor for real-time monitoring of sodium valproate.

*Microchem. J.* **2022**, 182.

(28) Elliott J R, H. D. A., The interaction of n-octanol with black lipid bilayer membranes. *Biochimica et Biophysica Acta (BBA)-Biomembranes*. **1979**, 557(1): 259-263.

(29) Ye, C. W.; Li, J., Density, Viscosity, and surface tension of n-octanol-phosphoric acid solutions in a temperature range 293.15–333.15 K. *Russ. J. Phys. Chem* **2012**, 86 (10), 1515-1521.

(30) Fumagalli L, E. A., Fabregas R, et al. Anomalously low dielectric constant of confined water. *Science*. **2018**, 360(6395): 1339-1342.

(31) Gao, H.; Wang, J.; Zhang, X.; Hu, M.; Xu, Q.; Xie, Y.; Liu, Y.; Lu, R., Confined lamellar channels structured by multilayer graphene for high-efficiency desalination. *Desalination*. **2022**, 530, 115981.

(32) Neek-Amal, M.; Peeters, F. M.; Grigorieva, I. V.; Geim, A. K. Commensurability Effects in Viscosity of Nanoconfined Water. *ACS Nano*. **2016**, 10, 3685-3692.

(33) Agmon, N.; Bakker, H. J.; Campen, R. K.; et al. Protons and Hydroxide Ions in Aqueous Systems. *Chem. Rev.* **2016**, 116, 7642-7672.

(34) Serowy S, Saparov S M, Antonenko Y N, et al. Structural proton diffusion along lipid bilayers. *Biophys.* **2003**, 84(2): 1031-1037.

(35) Zhang C, Knyazev D G, Vereshaga Y A, Ippoliti E, Nguyen T H, Carloni P, Pohl P. Water at hydrophobic interfaces delays proton surface-to-bulk transfer and provides a pathway for lateral proton diffusion. *PNAS*, **2012**, 109(25): 9744-9749.

(36) Slevin C J, Unwin P R. Lateral proton diffusion rates along stearic acid monolayers. *J. Am. Chem. Soc.* **2000**, 122(11): 2597-2602.

(37) Yang L, Zhao F, Zhao Y, et al. Enhanced exfoliation efficiency of graphite into few-layer graphene via reduction of graphite edge. *Carbon*, **2018**, 138, 390-396.

(38) Hu M, Yao Z, Wang X. Characterization techniques for graphene-based materials in catalysis. *Mater. Sci.*, **2017**, 4(3), 755-788.